LASER INTERFEROMETER GRAVITATIONAL WAVE OBSERVATORY
- LIGO -
CALIFORNIA INSTITUTE OF TECHNOLOGY
MASSACHUSETTS INSTITUTE OF TECHNOLOGY

Technical Note **LIGO-T2500241-x0-** 2025/09/24

PPLN Crystal Nonlinear Gain Measurements for Tabletop Waveguided Optical Parametric Amplification

Rana X. Adhikari, Peter G. Carney, Shruti Maliakal, Nora Dreslin

California Institute of Technology
LIGO Project, MS 18-34
Pasadena, CA 91125
Phone (626) 395-2129
Fax (626) 304-9834
E-mail: info@ligo.caltech.edu

Massachusetts Institute of Technology
LIGO Project, Room NW22-295
Cambridge, MA 02139
Phone (617) 253-4824
Fax (617) 253-7014
E-mail: info@ligo.mit.edu

LIGO Hanford Observatory
Route 10, Mile Marker 2
Richland, WA 99352
Phone (509) 372-8106
Fax (509) 372-8137
E-mail: info@ligo.caltech.edu

LIGO Livingston Observatory
19100 LIGO Lane
Livingston, LA 70754
Phone (225) 686-3100
Fax (225) 686-7189
E-mail: info@ligo.caltech.edu

http://www.ligo.caltech.edu/

Contents

1 Introduction

1.1 LIGO and Quantum Noise

LIGO (Laser Interferometer Gravitational-Wave Observatory) enables the detection and study of black hole mergers and neutron star mergers (and theoretically other astrophysical phenomena such as binary neutron star (NS) systems, asymmetric NSs, and a stochastic gravitational wave (GW) background) where matter is in conditions unachievable on even a scaled level, on Earth. The information detected with LIGO will give insight into how the laws of physics, especially of general relativity and nuclear physics, hold in the strong field regime, as well as potentially reveal new astrophysical phenomena and the physics of the early universe from before the cosmic microwave background [1] .

In order to detect gravitational waves from black hole mergers and other phenomena, LIGO has two Michelson interferometers positioned 2000 miles apart (10ms of light travel time). Each interferometer has 4km long arms whose lengths are changed when a passing gravitational wave moves a suspended mirror at the end of one interferometer arm on the order of $10^{-21}m$, causing a phase shift in one beam and therefore a change in power at the interferometer's readout. LIGO's strain sensitivity is best at 100Hz-1kHz, as shown in Figure 1 allowing us to detect strain on the order of $h = 10^{-23}$.

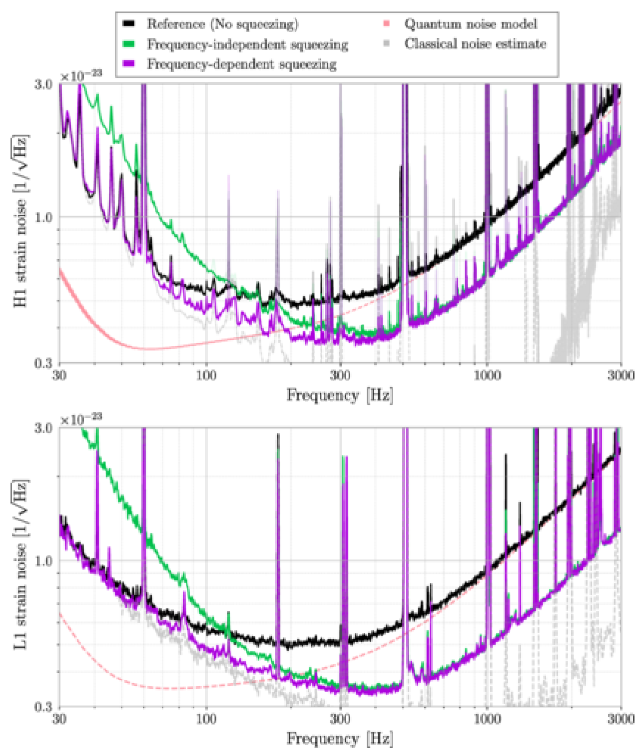

Figure 1: Advanced LIGO O4 run strain sensitivity with and without squeezing at Hanford and Livingston detectors. From [6]

At frequencies above this range, the shot noise of the laser causes phase noise due to the random (Poisson) distribution of the number of photons detected in a given time interval

[2]. The shot noise is given by

$$S = \sqrt{2\hbar P\nu}$$

where P is the average laser power and ν the laser frequency. At frequencies $< 100Hz$, radiation pressure noise (quantum back action) dominates because it causes low frequency oscillations in the mirrors due to the random variation of photon amplitude which results in force on the mirrors. Shot noise and quantum back action contribute to the overall noise level in LIGO which is a result of various environmental noises such as earthquakes and other vibrations. To limit noise and uncover these signals, we adopted a frequency-dependent quantum squeezing method with which we can squeeze uncertainty in phase to reduce noise at high frequencies and squeeze uncertainty in amplitude to reduce noise at low frequencies, at the cost of increasing noise in the other quadrature. This is achieved by generating vacuum state squeezed 1064nm light via spontaneous parametric down-conversion (SPDC) from a 532nm laser. This squeezed light is injected into LIGO at a frequency-dependent squeeze angle to reduce noise in the LIGO signal in the necessary quadrature for the GW frequency.

Waveguided optical parametric amplification (WOPA), aims to simplify the current squeezing method by generating squeezed light in a single pass through a periodically-poled Lithium Niobate (PPLN) crystal. This will limit possible losses that exist in the current optical parametric oscillator (OPO) cavity used for squeezing the LIGO signal. This project analyzes different aspects of the WOPA set up for tuning to improve the observed squeezing levels.

1.2 Quantum Squeezing

Light can be viewed as a quantum harmonic oscillator with two quadratures, in our case phase and amplitude, whose overall uncertainty must obey the uncertainty principle $\Delta x \Delta p \geq \frac{\hbar}{2}$. The squeezing parameter, r, determines the degree of squeezing in the given quadrature as shown below

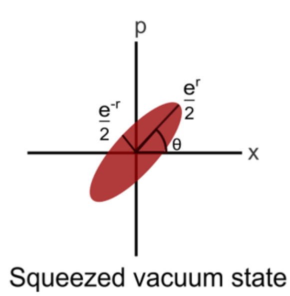

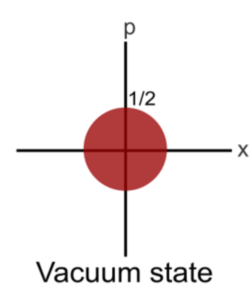

Figure 2: States of light in quadrature picture. The red area is the area of uncertainty of the state of light. Here r determines how much the squeezed and anti-squeezed quadratures are scaled. Both squeezed states here are phase squeezed because their uncertainty along the amplitude axis increases while the area along θ is decreased.

SPDC is a nonlinear optical parametric process in which a pump field (532nm in our case) interacts with vacuum fluctuations within a nonlinear crystal. This results in the conversion of a pump photon into a pair of signal and idler photons (1064nm) such that the frequencies of the signal and idler photons sum to the frequency of the pump in order to preserve energy and momentum.

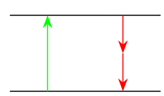

Figure 3: Energy level diagram of spontaneous parametric down conversion

We use type 0 SPDC where the polarizations of the pump, signal, and idler waves are equal. Because the polarizations and frequencies of the signal and idler photon pair are equal, they are indistinguishable and therefore coupled, since they were created at the same time. This coupling is the source of our squeezing, because the state of one photon within a pair must be exactly the state of its partner, the uncertainty in whichever quadrature we choose to squeeze the light is reduced.

This interaction between the vacuum and pump field in the crystal is enabled (amplified) by the second order nonlinear susceptibility tensor $\chi^{(2)}$ of PPLN, a dielectric medium, which has a significant value of $d_{33} = 25.3$ along its optical axis and allows for the contributions to the electric field of the E^2 terms in the following equation [5]

$$\tilde{P}(t) = \epsilon_0(\chi^{(1)}\tilde{E}(t) + \chi^{(2)}\tilde{E}^2(t))$$

where P is the polarization of the wave.

Parametric amplification is the process where, in addition to the pump beam, we also send a nonzero signal beam (1064nm) into the crystal. The pump wave then interacts with the signal in the crystal similarly to the vacuum fluctuations in SDPC and amplifies the signal wave by converting pump photons to pairs of signal and idler photons. We use this process to generate enough pairs of 1064nm photons to measure with our photodetectors (PD).

1.3 Measuring Squeezing

The level of squeezing for the squeezing parameter r is given by [3]

$$Sq(dB) = -10\log_{10}\left(\frac{\Delta X^2}{\Delta X^2_{vacuum}}\right)$$

Where $\Delta X = \frac{e^{-r}}{2}$ is the noise variance of the squeezed field in the chosen quadrature and $\Delta X_{vacuum} = \frac{1}{2}$ the noise variance of the vacuum state. To measure the noise variance of the squeezed field, we use a balanced homodyne detector (BHD) to combine the squeezed signal field and unsqueezed local oscillator (LO) field. The combined beam is split at a 50/50 beamsplitter and two beams differing in phase by $\frac{\pi}{2}$ are each sent to a PD as pictured in Figure 6. Therefore one PD measures the squeezed light and the other anti-squeezed light depending on which beam is aligned to the squeezed quadrature. As we modulate the phase of the LO beam with a piezo-mounted mirror, we also modulate the squeezing angle which determines the squeezed quadrature. For example, a relative phase of 0 between the beams relates to phase squeezing while a relative phase of $\frac{\pi}{2}$ produces anti-squeezing or amplitude squeezing.

To extract the squeezing level from the measured power of the squeezed and anti-squeezed light, we use a process illustrated by the below diagram

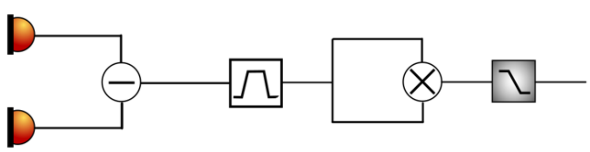

Figure 4: Signal processing of PD outputs for measurement of squeezing level. Diagram shows subtraction of signals, bandpass of difference, signal splitting and mixing, and then lowpass filter to extract fluctuations of shot noise.

Our goal is to measure the fluctuation in shot noise as a function of the squeezing angle so using the Multi Instrument Mode in the Moku:Pro we first gain balance and subtract the signals from the PDs. This will eliminate all power fluctuations that are at frequencies common to both PDs, such as the laser power fluctuating at the driving frequency. What remains is then the random fluctuations in power due to shot noise and the electronic noise in each PD. We then apply a bandpass filter to the subtracted signals to isolate shot noise and avoid contributions from electronic noise. We then digitally split this signal, take its root mean square, and isolate the low frequency DC signal of the shot noise fluctuation. The amplitude of these fluctuations gives the level of squeezing.

2 Nonlinear Gain

2.1 Methodology

In order to measure the nonlinear gain, we first align both the pump (532nm) and signal (1064nm) beams to the nonlinear axis of the crystal (which lies along the x-axis in the below figure, normally intersecting the ridge channel face noted) by adjusting the crystal position and signal path incoupling optics to maximize second harmonic generation of 532nm light from our 1064nm signal beam. The nonlinear axis is the path through the crystal

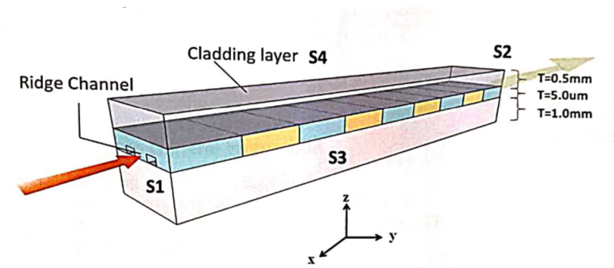

Figure 5: Diagram of PPLN waveguide from HC Photonics manual. The nonlinear axis normally intersects the face of the 2-3μm tall 6μm wide channel pointed out in the figure.

along which the nonlinear susceptibility, $\chi^{(2)}$, is greatest and therefore allows for the most contribution from the second order terms of a field passing through the crystal. Second harmonic generation (SHG) is another second order nonlinear process that is a result of this susceptibility. Optimizing this process will confirm that we are aligned to the nonlinear axis, along which all second order nonlinear processes occur in PPLN, and should therefore align the crystal for OPA. We use SHG to align to the crystal because the power output in SHG is higher than the output in SPDC. SHG is the stimulated emission of photons of power equal to the two photons converted to create it. SPDC is the conversion of one photon to two photons in a squeezed vacuum state from the interaction of the initial pump with vacuum fluctuations (0 average amplitude) and therefore has very low output power (pW range).

We then maximized the 532nm pump power measured after the crystal on a power meter by adjusting the crystal position (while maintaining SHG) and the 532nm path incoupling optics. This was done to get as much squeezing as possible because the output OPA power increases with increasing pump power. The maximum pump power while SHG was still observed was typically $4 \pm 1mW$. We then lowered the power of our signal beam so that $100\mu W$ of signal power was incident on the south(lower) PD shown in the WOPA setup diagram below.

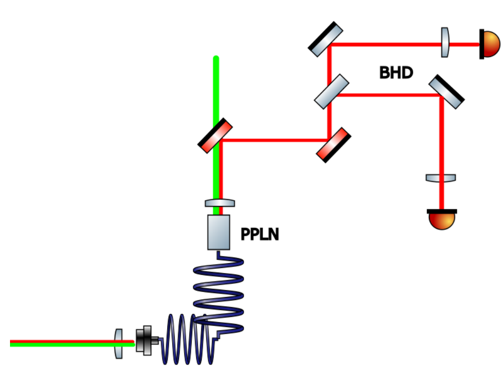

Figure 6: Simplified current WOPA experimental setup showing incoupling fiber, PPLN crystal, and focusing optics with Balanced Homodyne Detector (BHD)

To overcome potential phase mismatch between our input signal beam and the SPDC generated by the crystal, we drive a P-810.10 piezo from Physik Instrumente L.P. with a triangle wave from 0-15V at 30Hz using a function generator whose output is amplified by the MDT694B Piezo Controller. We adjust the voltage range and frequency until at least 2 peaks (1 wavelength) are seen within the overall sinusoid of the PD readout in one period of the driving function when both the signal and pump beams pass through the crystal. This corresponds to a triangle wave of 2Vpp with a 1mV offset from the function generator sent to the piezo driver, that has a gain of 7.5V/V. This ensures that we are driving the piezo such that the signal beam cycles through its phase at least once, so the signal and SPDC beams will be phase matched at least once in a period of the driving function. This oscillation between phase matching and mismatch of the signal and SPDC beams as the piezo moves can be seen in the following figure

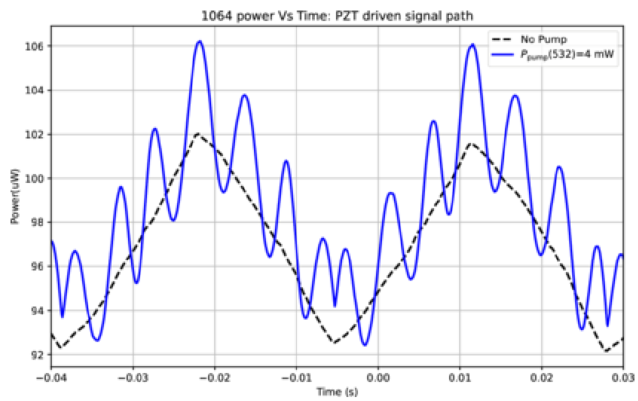

Figure 7: PD readout converted to W of signal beam with 0 and 4mW of pump power. The 0mW pump case shows the triangular oscillation we expect due to the change in fiber coupling as the piezo motion changes the path of the signal beam. The 4mW case shows the oscillations from the interaction of SPDC output and the seed signal beam atop this underlying low frequency oscillation.

The oscillations within the triangle wave at max pump power in the above figure show the constructive and destructive interference of the input signal beam and the output of nonlinear process which has the same phase as the pump beam. Therefore the amplitude of these oscillations is the power output in OPA, ie. the parametric amplification of the input signal beam. We calculate the nonlinear gain from our data by fitting and subtracting the overall triangle wave and then taking the ratio of the amplitude of these smaller oscillations to the overall average power of the remaining function.

2.2 Squeezing Level Calculation

In order to calculate our expected level of squeezing from the nonlinear gain we measure from OPA, we follow the theory described in chapter 2 of [7]. The squeezing operator in the 'quadrature picture' is expressed as the diagonal matrix

$$H_s = \begin{pmatrix} e^r & 0 \\ 0 & e^{-r} \end{pmatrix}$$

where r is the squeezing parameter and the first row represents the anti-squeezed quadrature, the second the squeezed quadrature. The rotation matrix R_ψ

$$R_\psi = \begin{pmatrix} \cos\psi & \sin\psi \\ -\sin\psi & \cos\psi \end{pmatrix}$$

transforms our initial state into the quadrature picture and back, and is dependent on the squeezing angle ψ between the squeezed field and the local oscillator (LO). In our nonlinear gain experiment this angle is the phase difference between the pump and the input signal beams which we modulate with the piezo. The effect of squeezing on our initial state (the input signal beam) can be represented as

$$\begin{pmatrix} b_1 \\ b_2 \end{pmatrix} = R_\psi H_s R_\psi^\dagger \begin{pmatrix} a_1 \\ a_2 \end{pmatrix}$$

where we let $a_1 = \alpha\cos 0 = \alpha$, $a_2 = \alpha \sin 0 = 0$ so that our phase difference or squeezing angle is measured with respect to the input signal field. We see that our output state is

$$\begin{pmatrix} b_1 \\ b_2 \end{pmatrix} = \begin{pmatrix} \alpha e^r \cos^2\psi + \alpha e^{-r}\sin^2\psi \\ \alpha e^r \sin\psi\cos\psi - \alpha e^{-r}\sin\psi\cos\psi \end{pmatrix}$$

To calculate the expectation value of the photon number of our squeezed state, which is proportional to the power, we take

$$b_1^2 + b_2^2 = \alpha^2(\cosh 2r + \cos 2\psi \sinh 2r)$$

This is an oscillatory function of the squeezing parameter, the input signal field amplitude, and squeezing angle which is proportional to the output power of OPA. We can use this with the measured value of OPA power from our nonlinear gain data to solve for r, the squeezing parameter, and then calculate our expected level of squeezing using the equation from the Introduction

$$Sq(dB) = -10\log_{10}(e^{-2r})$$

2.3 Nonlinear Gain Measurement

Using the approach described in the Methods section, we measure the nonlinear gain as a function of pump power

The figure below shows the expected square root dependence on the pump power of the nonlinear gain seen in second order nonlinear optical phenomena of approximately $0.5\text{dB}/\sqrt{W_{pump}}$. We fit our measured power during OPA at various pump powers to the squeezed photon number function derived in the previous section to solve for the squeezing parameter r, and calculate the expected squeezing level. We measure an initial maximum gain of 0.12dB for 4mW of pump power which corresponds to the previously measured maximum squeezing level of 0.13dB. This confirms that our method of calculating squeezing level from nonlinear gain is accurate and that we can tune this nonlinear gain in order to increase squeezing.

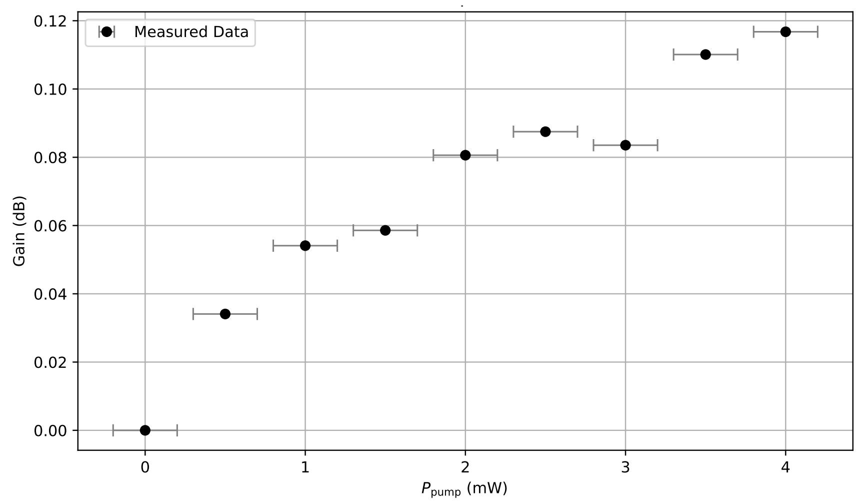

Figure 8: Nonlinear gain in dB as a function of pump power calculated from the ratio of OPA peak power to average power

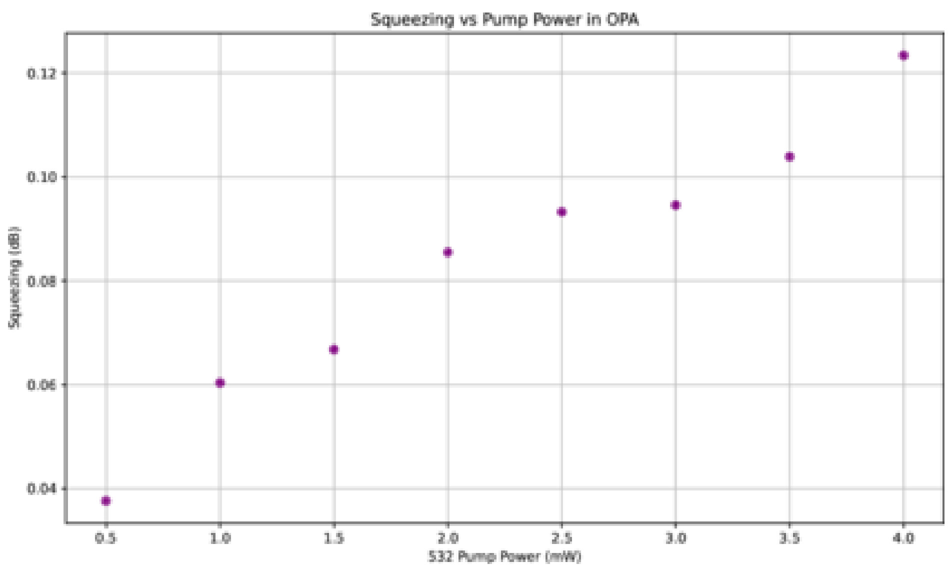

Figure 9: The expected squeezing level calculated from observed nonlinear gain of OPA as a function of pump power.

We can extrapolate our data to predict squeezing parameters values and squeezing levels possible in the system for higher pump powers as shown in the following figure.

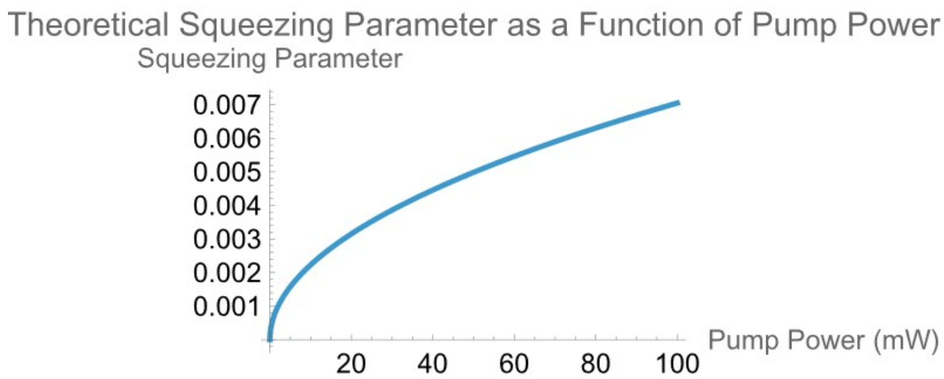

Figure 10: Predicted squeezing parameter values up to maximum power tolerated by crystal calculated from measured OPA power.

These values correspond to the squeezing levels possible within our system, assuming perfect BHD visibility. We can use this as a benchmark to compare our measured data and inform our tuning or modification of the system to improve squeezing.

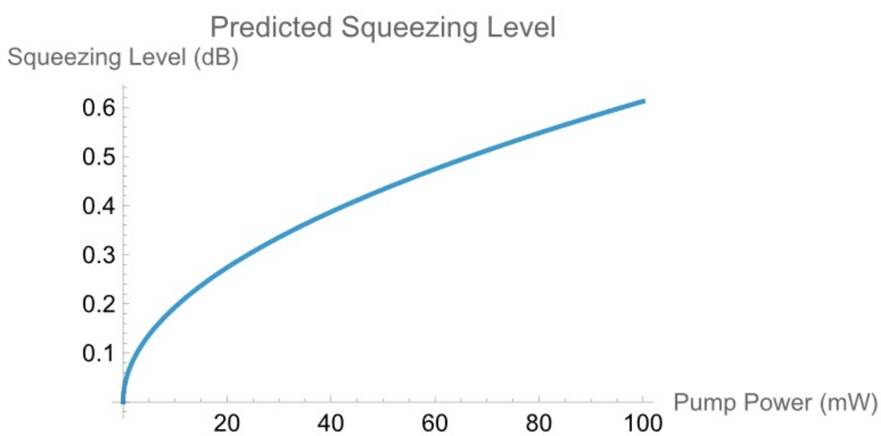

Figure 11: Predicted squeezing levels calculated from projected squeezing parameter up to maximum pump power tolerated by crystal.

3 Polarization

3.1 Methodology

To maximize the nonlinear gain and therefore the squeezing level, we adjust the polarization of the pump and signal beams first to vertical, the optimal polarization cited in the PPLN manual, and then we tune the polarization of both beam to maximize the amplitude of the oscillations associated with OPA. We measure the polarization by placing a PBS in the beam path before the incoupling fiber and after any other polarizing or polarization filtering optics as shown below

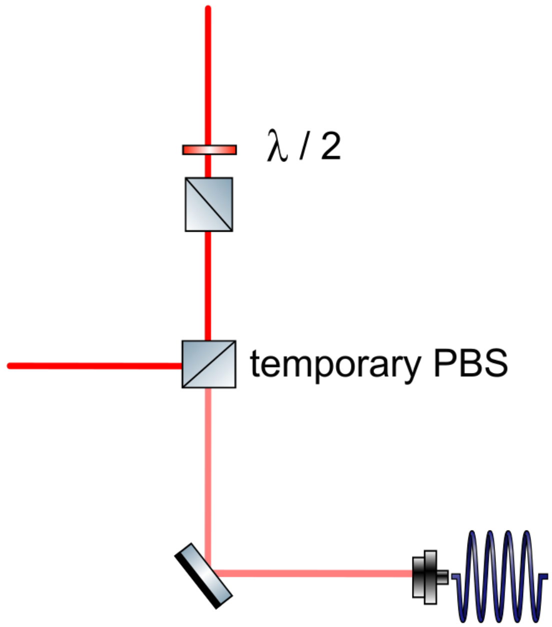

Figure 12: Simplified polarization measurement setup in 1064nm beam path before fiber to crystal.

The PBSs we used reflect vertically polarized light and transmit horizontally polarized light so we set up a power meter in the beam path and adjusted the angle of the permanent PBS to minimize the measured power transmitted through the temporary PBS. After both beams' polarizations were made as vertical as possible, the temporary PBSs were removed and we set the pump power to a maximum of 3.9mW measured after the crystal and adjusted the signal power such that 50μW was incident on the PD. We then drove the piezo in the signal path with a 30Hz triangle wave from 0-15V and measured the peak to peak value of the oscillations due to the interaction of the input signal and SPDC beams. We tuned the polarizations of the signal and pump beams to maximize this peak to peak value (and the nonlinear gain) by adjusting the angle of the final PBS in each path. This limits loss due to polarization mismatch between the beams and the crystal axis.

We measure the polarization drift of both the pump (532) and signal (1064) beams to ensure the increase in gain we see with increasing pump power is solely due to the pump power increase and not the polarizations of the beams drifting over time to better align to the crystal or each and increase OPA power output. For the 1064 beam, we set up a PDA10CS at the outputs of the PBS in a picked off path pictured below to measure the powers of the s (vertical) and p (horizontal) polarizations separated by the PBS. This PBS also reflects s-polarized light and transmits p-polarized light. We first aligned the PDs by eye and then with the oscilloscope in the Moku:Pro to get a readout of 10mV for ∼32µW as measured with the power meter at the s-PD and ∼151mV for ∼1.55mW at the p-PD. We used a conversion of 1mV=10µW for the signal beam data based on the power measured via power meter at the PD sensor and the corresponding readout. We used the data logger in the Moku:Pro to record the PD readouts over an hour.

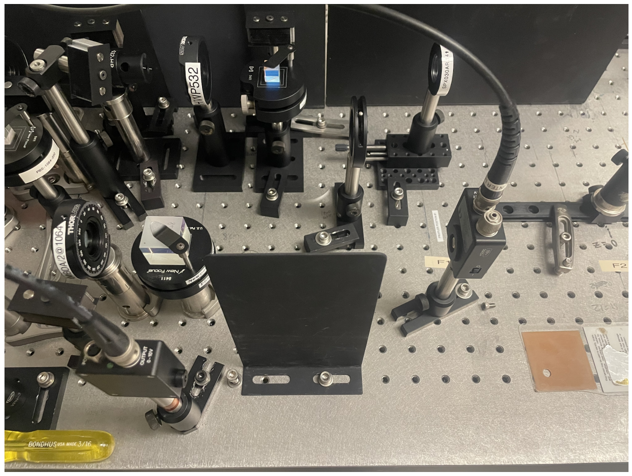

Figure 13: Signal path polarization drift setup with a PD at each output of the PBS

For the 532 beam, we used the same PDs even though their sensitivity range is 900-1700nm because there were no PDs available in the range of 532nm. As pictured below, we used a PBS101 in the pump path after the first mirror with the iris closed enough to limit the power into the PBS below 70mW so as to not damage the PDs

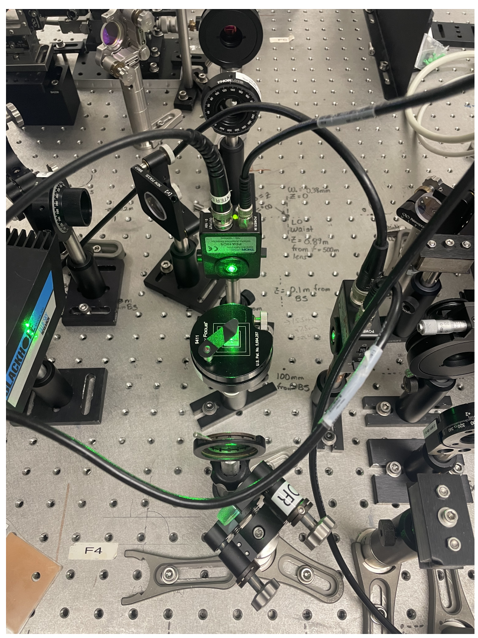

Figure 14: Pump beam polarization drift measurement set up

A nearly identical data collection method to that for the 1064 beam was followed. The PD in the p path read 1.727V for 67.6mW of 532 so we used a conversion of 25.55mV=1mW. The PD in the s path read 54.5mV for 2.83mW of 532 so we use a conversion of 19.26mV=1mW. We use these slightly different conversion factors for the two PDs because they are not designed to have reliable responses at this wavelength and we avoid generalizing this unpredictable value between the PDs.

3.2 Polarization Tuning and Drift Measurement

Our first approach to increase nonlinear gain was to tune the polarizations of the signal and pump beams as described in the Methods section. We began by minimizing the ratio of horizontal to vertical polarization in the beams to 0.00027 in the pump beam and 0.0043 in the signal beam. We then measured the output power of OPA while driving the signal beam. Initially, after maximizing the vertical polarization in both beams, which is cited as the optimal polarization to align to the nonlinear axis of the crystal, we saw a mean peak to peak value of 8.75μW over $\sim$ 2000 counts. We adjusted the polarizations of the pump and signal beams by changing the angle of the final PBS in their respective paths before the fiber while also adjusting the angle of the polarization axis of our fiber in order to maximize this peak to peak value corresponding to the power increase due to OPA. This peak to peak value, and therefore the nonlinear gain, was maximized to a mean of 10.8μW. The horizontal to vertical polarization ratios of the signal and pump beams were then measured to determine what polarization resulted in the maximal nonlinear gain. The optimal ratios were 0.00037 in the pump beam and 0.0046 in the signal beam, an increase of 0.0001 and 0.0002 respectively. This suggests that the fiber is likely not maintaining the polarization of the beams or that the crystal's axis is not optimally aligned to a purely vertically polarized beam.

We then measured the polarization drift of both the signal and pump beams as described in the Methods section. The polarization angle was calculated as a function of time by

$$\theta = \frac{1}{2}\arccos\frac{P_p - P_s}{P_p + P_s}$$

where P_p and P_s are the powers of the horizontally and vertically polarized components of the beam, respectively. This formula accounts only for change in power due to polarization drift and not overall laser power fluctuations because any total power fluctuation would be present in both polarization components and cancel. The polarization drift in the beams over an hour can be seen in the following graphs

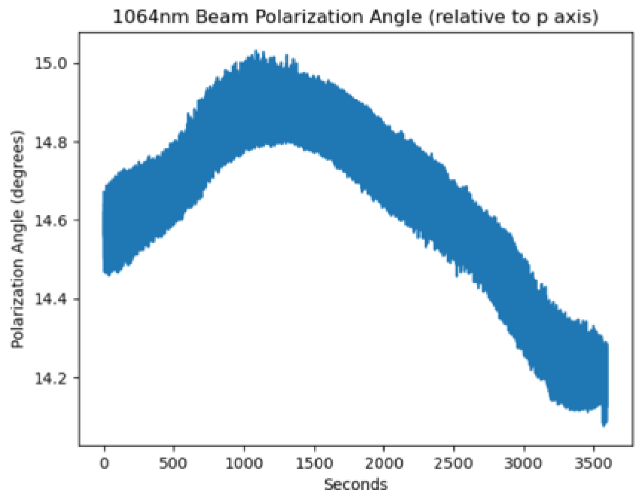

Figure 15: The polarization drift with respect to horizontal polarizationin the signal beam as a function of time over an hour

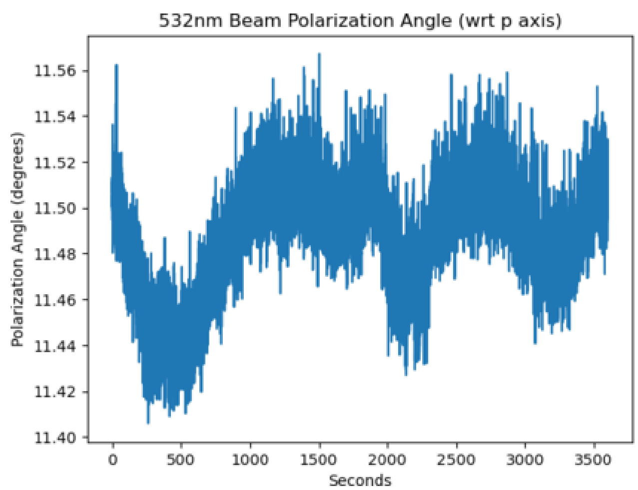

Figure 16: The polarization drift with respect to horizontal polarization in the pump beam as a function of time over an hour

Both beams drift less than 1 degree in an hour which is not significant enough to affect our gain measurements due to an overall change in power from the polarizations drifting into or out of alignment with the fiber or crystal. This is further confirmed by calculating the angle drift density as a function of frequency We used the Matlab psd function to transform the data from Figures 10 and 11. The 532 beam polarization is stable and only shows a low 10^{-5} resonance around 20Hz which is not of the order that will affect our measurements. The 1064nm beam polarization is less stable than the 532 but the fluctuations are not of the order that would affect our nonlinear gain measurements. This confirms that there are no significant polarization fluctuations which could affect our nonlinear gain data at the frequency we drive the signal beam's phase. Additionally, this confirms that we were able to increase the nonlinear gain by 0.05dB or 4.25% by tuning the polarization.

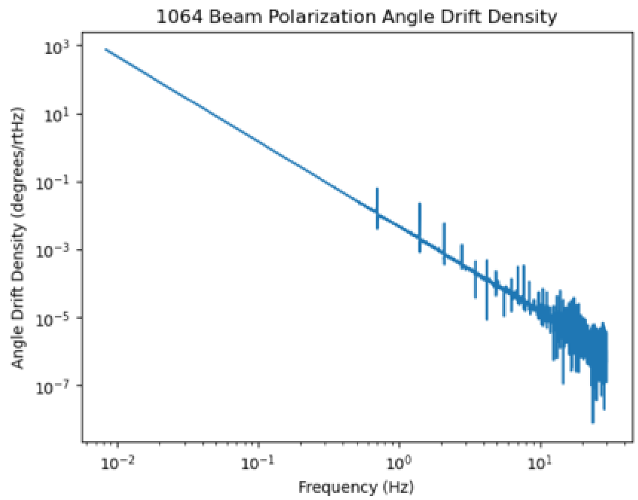

Figure 17: Signal beam polarization angle drift density with respect to horizontal

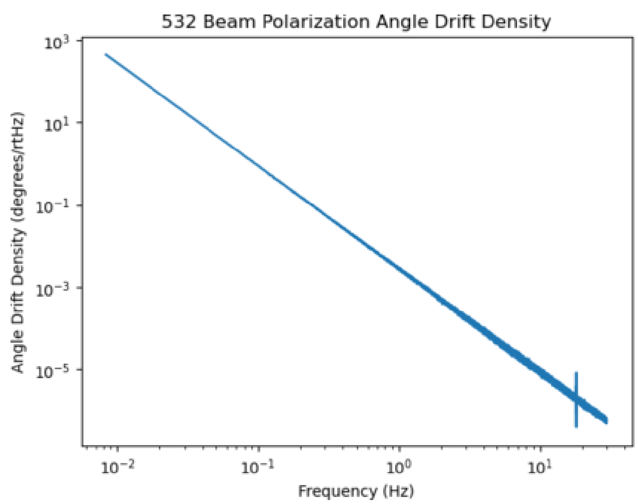

Figure 18: Pump beam polarization angle drift density with respect to horizontal

4 Mode Matching

4.1 Piezo Characterization

Before we began profiling the signal beam for our modematching calculations, we first replaced a curved mirror mounted on a piezo in the signal path with a flat turning mirror also mounted on a piezo to reduce astigmatism in the beam. Since we use this piezo to drive the signal beam during our nonlinear gain measurements, we have to characterize the response of the piezo to a driving voltage. This was done by constructing a Michelson interferometer in the signal path with a 50/50 beamsplitter, a 1025 AR-coated flat mirror, the flat mirror mounted on the piezo, and a PDA10CS photodetector.

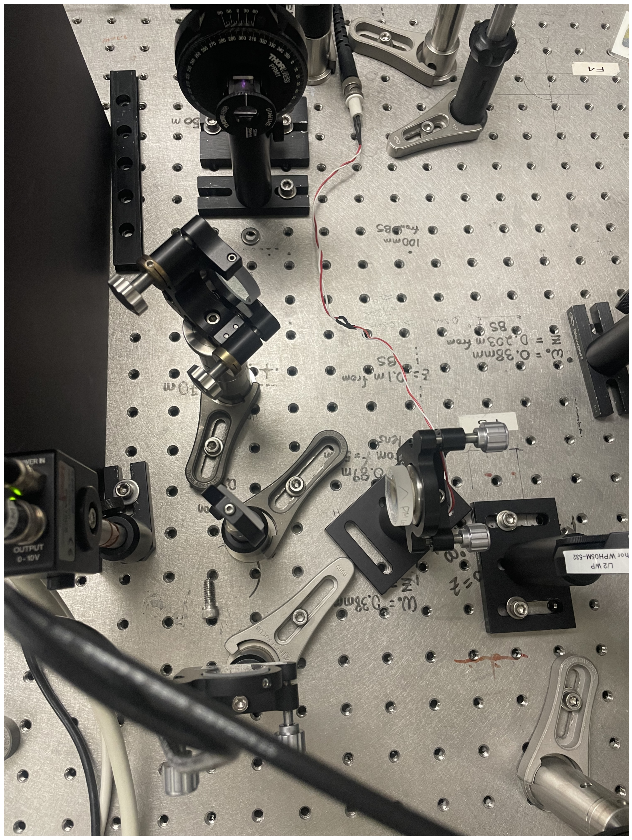

Figure 19: Temporary Michelson interferometer in signal path for characterization of piezo response.

The piezo response to a 0-7.5V triangle wave was tested at 30, 50, and 100Hz. 100Hz gave the clearest response on the PD in both time and frequency domains so we used this frequency to measure the response. The piezo driver was set to its 15 gain setting, allowing for a maximum of 150V to be sent to the piezo. We drove the piezo with with triangle waves of increasing peak to peak voltages until even integer number of peaks were seen within one period (10ms) of the driving function. Two peaks corresponds to the piezo moving one wavelength because the modulated and unmodulated beams maximally constructively interfere twice.

Two peaks were seen when for a driving voltage range of 0-67.5V and four peaks were seen for a driving voltage range of 0-135V. Using scipy, the data taken with the PD during at these driving amplitudes was fit to sinusoids to calculate their frequencies.

Based on the frequencies of the fit sinusoids, 206.25Hz and 412.5Hz, the response appears linear up to 0.0001. These frequencies correspond to a response of 1 wavelength (1064nm) of movement for 64.45V ($\pm$0.001V).

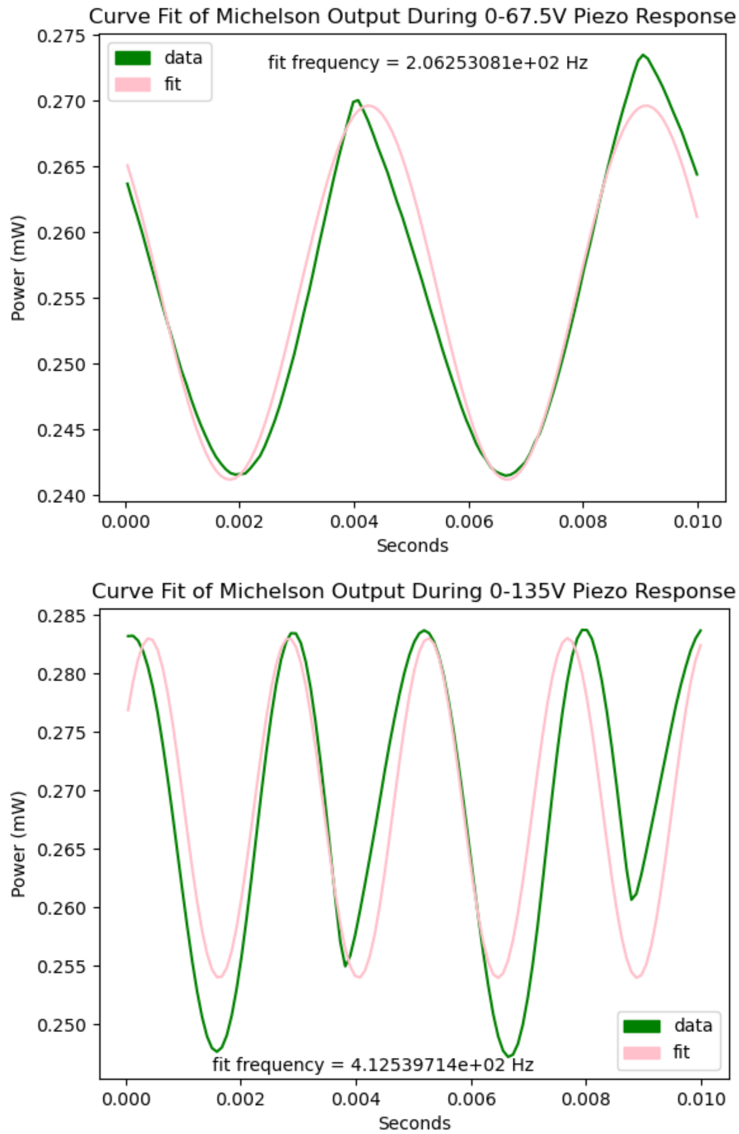

Figure 20: Sinusoidal curve and frequency fits of piezo response data

4.2 Methodology

The main method by which we tune the squeezing level is mode matching; whether it be into the crystal itself, the incoupling fiber, or the BHD. In order to optimize the mode matching to the crystal, we tried various incoupling setups with different types of fiber and with free space coupling. This incoupling to the crystal is our main source of loss in the system with up to 90% loss observed from the fiber incoupling through the crystal. We assume trivial absorption in the crystal because it is designed to be transparent at the pump and signal wavelengths, so we look to the fiber and crystal coupling to reduce loss. Three fibers were tested to maximize pump power; the initial PM fiber AR coated for 1064nm light, a PM APC/PC fiber AR coated for 532nm light (P3-488PM-FC-1), and a single mode fiber coated for 532nm light (P4-460AR-2). Bare fiber coupling to the crystal was used for all fibers in order to get the output beam as close to the fiber face as possible before it diverged due to its high NA. The mode field diameter (MFD) of the crystal is $4.83\mu m \times 4.16\mu m$ and the new fibers we tested have MFDs of 3.3 ± 0.5 µm at 515 nm for the P3-488PM-FC-1 and 2.8 - 4.1 µm at 488 nm for the P4-460AR-2 which should allow all the light from the fiber to couple into the crystal. To test free space coupling, we use various combinations lenses to focus the beam to the MFD of the crystal and maximize SHG power to confirm alignment.

To couple as much light as possible into the fibers (and crystal) we profile the pump beam, taking measurements in centimeter increments around the waist, to calculate its q parameter and then use ABCD matrices to find a lens solution. We look for a two lens solution that will focus the beam down to the MFD of the fiber (or crystal) and use Mathematica to define the beam size as a function of the focal lengths and the distance between the lenses.

4.3 Results

The following is one of the lens solutions we obtained;

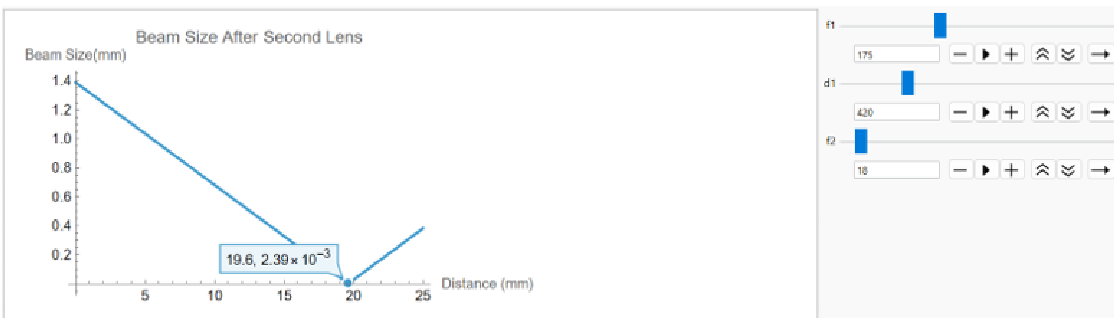

Figure 21: Lens solution for focal lengths of lenses (f1=175mm, f2=18mm) and distance between lenses (d1=420mm). This lens combination allows for the beam to have a waist of 2.39μm, which is small enough for free space coupling into the crystal.

We tested multiple lens solutions which focused the beam waist below 5μm and confirmed that this process result was accurate and repeatable with a DataRay Beam'R2 beam profiler (sensitive to $1\mu m^2$). This shows that free space coupling into the waveguide is possible, which could eliminate the 90% power loss we see through the fiber and improve our squeezing levels. We then attempted free space coupling into the waveguide and observed SHG up to 100μW.

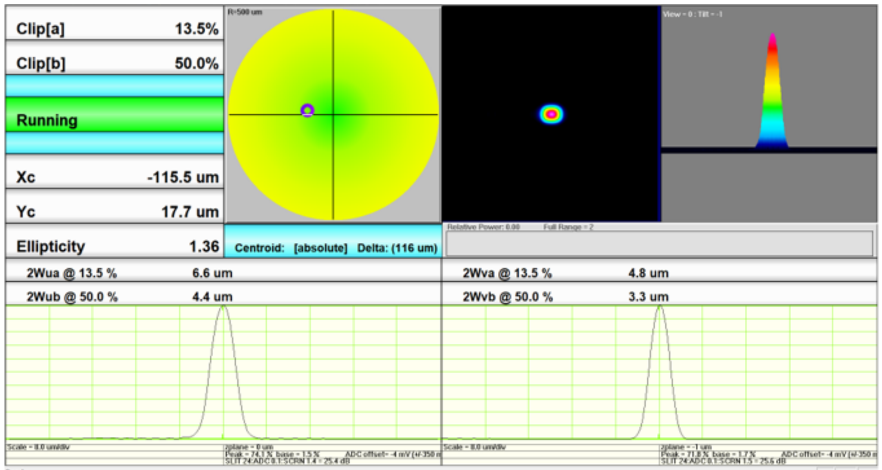

Figure 22: Beam profiler readout showing beam spot focused to a horizontal radius of 4.8μm and a vertical radius of 6.6μm. Note that this measurement was likely not taken at the waist of the beam because the beam profiler was placed by hand. The beam also has a very short Rayleigh range, implying that the true beam waist is likely smaller than this measured beam spot.

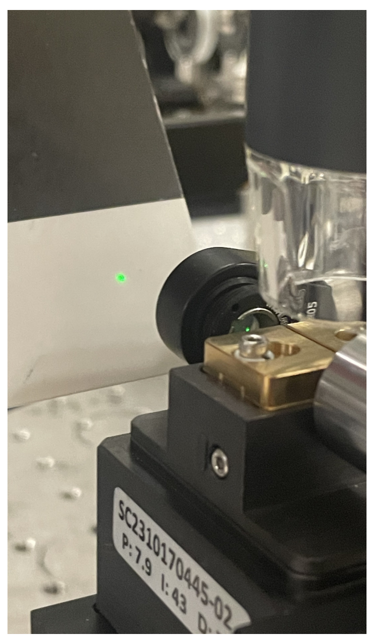

Figure 23: SHG achieved with free space coupling

This is a significantly lower conversion efficiency than that previously seen with the original 1064nm coated PM fiber (100μW for 25mW of 1064). Despite the potential elimination of fiber losses, we chose not to continue our free space coupling attempt in the interest of time. We instead settled on a modified version of the original setup, using the 1064nm AR-coated PM fiber now oriented with no curves to reduce strain. We use a 500mm focal length lens 170cm before the fiber coupling, a 125mm focal length lens 70cm before the fiber coupling, and a 40x adjustable objective which should focus the beam waist to $< 1\mu$m, maximizing the power going into the fiber.

Figure 24: Final incoupling setup using recut original fiber oriented straight into waveguide to reduce stress and loss.

With this setup, we saw up to 6.6mW of pump power through the crystal while aligned for SHG. We then aligned the BHD by adjusting the aspheric lens immediately after the waveguide and the turning mirrors leading to the BHD to mode match the signal beam to the LO beam. This was done by walking the beam and using the Beam'R2 to compare the beam spots of both the LO and signal beams at two places along an arm of the BHD. After minimizing ellipticity and overlapping the beams as much as possible, we measured an improved BHD visibility of 62%. Greater BHD visibility will allow for more squeezing to be measured and therefore increase the impact that the tuning of different aspects of the system has on the squeezing level.

5 Future Steps

We plan to lock the phase of the signal to the pump beam in order to maximize nonlinear gain, but the phase 532nm pump itself drifts noticeably overtime and the power fluctuates significantly which could affect our measurement of output OPA power. The laser's 532nm power has been increased as much as possible without realigning the SHG cavity within it, but the cavity is currently very sensitive. We plan to realign and stabilize the laser cavity to increase pump power and stabilize the pump beam phase.

To improve our nonlinear gain and therefore our squeezing levels, we plan to first alter the path of the signal beam to eliminate the underlying triangle wave from our data. This triangle wave is caused by the beam coupling and decoupling to the fiber as the piezo changes its path in the plane of the fiber couple. In the planned configuration, the signal beam will be normally incident on the piezo-mounted mirror so its transverse position will be unaffected by piezo movement.

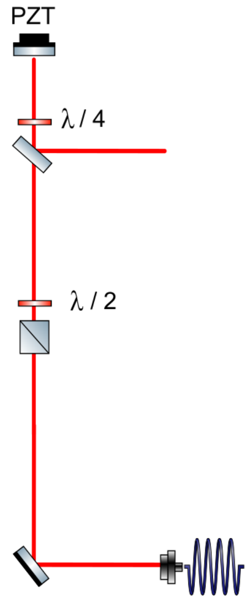

Figure 25: Planned signal path which will eliminated piezo's effect on fiber coupling. The beamsplitter reflects vertically polarized light through the quarter waveplate which then reflects off of the mirror. This reflected light again passes through the quarter waveplate, becomes horizontally polarized, and can then pass through the beamsplitter to continue down the signal path.

The main result of this project is the demonstration that free space coupling into the waveguide is possible. Successful free space coupling should drastically increase the pump power through the crystal and therefore improve squeezing levels. Our next steps would be to test lens solutions which focus the pump beam within the MFD of the waveguide and then maximize nonlinear gain.

6 Acknowledgements

I'd like to thank my mentors, Peter Carney and Shruti Maliakal, for all their help and guidance along with Professor Adhikari and everyone else in the lab. My lab partner, Tanisha Ray, contributed significantly to much of the work described, especially in the Nonlinear Gain section. I'm very appreciative of Caltech and LIGO for hosting this program. This project was funded by the NSF.

References

[1] B P Abbott et al *LIGO: The Laser Interferometer Gravitational-Wave Observatory* 2009 Rep. Prog. Phys. 72 076901

[2] Wenxuan Jia et al. ,Squeezing the quantum noise of a gravitational-wave detector below the standard quantum limit. Science385,1318-1321(2024).DOI: 10.1126/science.ado8069

[3] HC Photonics Corp., "Key factors/Critical requirements and PPLN for squeezing applications". V. Jan-25, p1

[4] Schubert, M., & Wilhelmi, B. (1986). *Nonlinear Optics and Quantum Electronics*. John Wiley & Sons, Inc.

[5] Boyd, R. (2020). *Nonlinear Optics (Fourth edition)*. Academic Press. https://doi.org/10.1016/B978-0-12-811002-7.00010-2

[6] LIGO O4 Detector Collaboration. (2023). *Broadband Quantum Enhancement of the LIGO Detectors with Frequency-Dependent Squeezing*. American Physical Society. https://link.aps.org/doi/10.1103/PhysRevX.13.041021

[7] Ganapathy, Dhruva. (2024). *Expanding the Reach of Quantum Enhanced Gravitational-Wave Detectors*.